An 8-channel receive array for improved ^{31}P MRSI of the whole brain at 3T

Journal:	*Magnetic Resonance in Medicine*
Manuscript ID	MRM-18-19428.R2
Wiley - Manuscript type:	Note
Date Submitted by the Author:	21-Feb-2019
Complete List of Authors:	van Uden, Mark; Radboud university medical center, Radiology and Nuclear Medicine Peeters, Tom; Radboud university medical center, Radiology and Nuclear Medicine Rijpma, Anne; Radboud university medical center, Department of Geriatric Medicine; Radboud university medical center, Radboudumc Alzheimer Center, Donders Institute for Brain, Cognition and Behaviour Rodgers, Christopher; University of Cambridge, Wolfson Brain Imaging Centre Heerschap, Arend; Radboud university medical center, Radiology and Nuclear Medicine Scheenen, Tom; Radboud university medical center, Radiology and Nuclear Medicine
Research Type:	arrays < RF Coils < Instrumentation < Technical Research
Research Focus:	Normal < Anatomy < Brain < Neurological

An 8-channel receive array for improved ^{31}P MRSI of the whole brain at 3T

Mark J. van Uden[1], Tom H. Peeters[1], Anne Rijpma[2,3], Christopher T. Rodgers[4], Arend Heerschap[1], Tom W.J. Scheenen[1,5]

[1] Department of Radiology and Nuclear Medicine, Radboud university medical center, Nijmegen, The Netherlands

[2] Department of Geriatric Medicine, Radboud university medical center, Nijmegen, The Netherlands

[3] Radboudumc Alzheimer Center, Donders Institute for Brain, Cognition and Behaviour, Radboud university medical center, Nijmegen, The Netherlands

[4] Wolfson Brain Imaging Centre, University of Cambridge, Cambridge, United Kingdom

[5] Erwin L. Hahn Institute, University Hospital Duisburg-Essen, Essen, Germany

Corresponding author:

Mark J. van Uden, Radboud university medical center, Department of Radiology and Nuclear Medicine, Geert Grooteplein-zuid 10, huispost 766, P.O. Box 9101, 6500 HB Nijmegen, Email: Mark.vanuden@radboudumc.nl, T: +31 24 365 2285, F: +31 24 354 08 66

Manuscript type: note

Word count: 2793
Number of figures: 5

Abstract

Purpose: To demonstrate a $^{1}H/^{31}P$ whole human brain volume coil configuration for 3T with separate ^{31}P transmit and receive components that maintains ^{1}H MRS performance and delivers optimal ^{31}P MRSI with ^{1}H decoupling.

Methods: We developed an 8-channel ^{31}P receive array coil covering the head, to be used as an insert for a commercial double-tuned $^{1}H/^{31}P$ birdcage transmit-receive coil. This retains the possibility of using low power rectangular pulses for ^{1}H-decoupled 3D ^{31}P MRSI (nominal resolution 17.6cm^3; acquisition duration 13min), but increases the signal-to-noise ratio (SNR) with the receive sensitivity of ^{31}P surface coils. The performance of the combined coil setup was evaluated by measuring ^{1}H and ^{31}P SNR with and without the ^{31}P receive array and by assessing the effect of the receive array on the transmit efficiencies of the birdcage coil.

Results:

Compared to the birdcage coil alone, the ^{31}P insert in combination with the birdcage achieved an average ^{31}P SNR gain of 1.4 ± 0.4 in a center partition of the brain. The insert did not cause losses in ^{1}H MRS performance and transmit efficiency, whereas for ^{31}P approximately 20% more power was needed to achieve the same $\gamma B1$.

Conclusion: The new coil configuration allows ^{1}H MRSI and optimal ^{1}H-decoupled 3D ^{31}P MRSI with increased SNR of the human brain without patient repositioning, for clinical and research purposes at 3T.

Keywords: Brain, ^{31}P MR spectroscopic imaging, RF array coil, 3 Tesla, ^{1}H-decoupling,

Introduction

In vivo phosphorus MR spectroscopy (^{31}P MRS) of the brain allows to non-invasively measure brain metabolites that are linked to the energy and phospholipid metabolism. It is used to study several neurological diseases and other pathologies like cancer in which metabolite levels are altered [1, 2].

Although the unique value of ^{31}P MRS in the non-invasive examination of brain diseases has already been demonstrated for this purpose many years ago (e.g.[3, 4]), it is much less used than ^{1}H MRS [5], mainly because of a lower sensitivity and the need for additional hardware. To obtain localized ^{31}P MR spectra of the human brain it is common to employ a birdcage-type of coil for transmit/receive with either a single or multi-voxel MR spectroscopic imaging (MRSI) pulse sequence [6, 7]. For anatomical guidance by MRI and B_0-shimming it is required that the ^{31}P coil is integrated with a ^{1}H RF element, which can also be used for ^{1}H-decoupling, inducing the nuclear Overhauser effect (NOE) and ^{1}H MRS.

To overcome that low signal-to-noise (SNR) hampers quantification of metabolite peaks, the lower sensitivity of ^{31}P MRS compared to ^{1}H MRS can be compensated by prolonging acquisition times, enlarging voxels and/or using a higher magnetic field. However, sensitivity can also be enhanced by reducing the size of the receiving RF coils, in particular at the more superficial regions of the brain [8]. Multiple small receive elements arranged in a 2D or 3D array will result in an SNR increase while maintaining a large field of view (FOV). Receive arrays are particularly attractive in combination with a homogeneous transmit coil. This enables uniform excitation across the FOV by excitation with low power radiofrequency (RF) pulses instead of adiabatic pulses with large power deposition in the tissue, the latter resulting in a high specific absorption rate (SAR). This leaves room in ^{31}P experiments to apply RF-pulses for ^{1}H-decoupling and/or inducing NOE for increased spectral resolution and SNR, respectively.

Since 3T systems are widely available in the clinic, many sites could take advantage of an improved coil design rather than switching to expensive ultra-high field (≥ 7T) systems. Even though X-nuclei phased array coils are not new [9-11], to our knowledge, a ^{31}P phased array coil insert to be used in combination with a commercially available ^{1}H/^{31}P birdcage coil has not been designed for the brain at 3T.

In this work we aimed to maximize SNR and spectral resolution and thereby the applicability of ^{31}P MRS at 3T, by developing a dedicated 8-channel ^{31}P receive head-array coil that can be used

in combination with a $^{1}H/^{31}P$ birdcage transmit-receive coil to enable ^{1}H-decoupling and NOE. We acquired *in vivo* ^{31}P spectra of the brain and compared the performance of the coil setup with and without the ^{31}P 8-channel insert.

Methods

Coil design

An 8-channel ^{31}P receive head-array coil was designed to be combined with a commercially available quadrature Tx/Rx $^{1}H/^{31}P$ birdcage coil (RAPID Biomedical GmbH, Rimpar, Germany). Both coils were actively detunable at the ^{31}P frequency. To this end, the commercial coil had to be adjusted by the manufacturer. For ^{1}H applications the birdcage coil was always used to both transmit and receive.

The elements of the head-array were constructed using 12.7 mm wide copper tape with a thickness of 35.6 µm on a Plexiglas former with an outer diameter of 24.5 cm. The dimensions of the elements were 100 by 200 mm, except for the frontal element (100 by 100 mm) to create space for the patient's nose and view, herewith improving patient comfort (Fig. 1). The loaded and unloaded Q-factors of the elements and element coupling (S21) were measured on the workbench with a vector network analyzer (R&HZVL3, Rohde & Schwarz, Munich, Germany). Adjacent elements, separated by a gap of 0.5 cm, were isolated from each other by means of capacitive decoupling [12]. Furthermore, all elements were isolated by preamp decoupling [13]. Two active ^{31}P detuning circuits as well as two ^{1}H traps [14] per element prevented coupling between the transmit field and the receive elements which could otherwise have produced hotspots with high local SAR. The cables of the receive array were connected to an interface box which was intentionally positioned behind the setup to keep distance between the transmit coil and receive circuits. To prevent ^{1}H power loss, four cables were equipped with additional ^{1}H cable traps.

Interface box

The interface box contains low input impedance preamplifiers, phase shifters and ^{1}H tank circuits. The matching circuit used to introduce preamplifier decoupling as proposed by Roemer et al. [13] requires the low input impedance from the preamplifier at its ports. This was achieved by a 180 degree phase shift between the input from the preamplifier and the matching circuit. The phase shift was a cumulative effect of the cable, the cable traps and phase shifters (Fig. 2). Note that no attempt was made to adjust the relative phase of the receive elements in hardware. This is because the MR system receives and digitizes all channels separately, and then in

software deduces the appropriate weights for optimal signal combination using the whitened singular value decomposition (WSVD) algorithm [15].

The functionality of this circuitry setup was confirmed on the workbench by means of S21 measurements using two isolated pickup probes. ^{1}H tank circuits prevented the ^{31}P spectra from contamination with spurious signals during ^{1}H-decoupling. Coil files were adjusted for automated coil detection and proper coil control by the MR system.

Measurements

As the presence of the ^{31}P head array coil in the ^{1}H/ ^{31}P birdcage coil might influence the transmit fields locally and therefore could exceed SAR limits, we performed temperature measurements on phantoms placed in the combination of both coils with maximum transmit power on the birdcage coil. Since the commercial birdcage coil is CE-approved with characterized global SAR levels, we verified that insertion of the phased array coil would not result in local SAR hotspots exceeding these approved levels. The load of a human head was mimicked by a cylindrical phantom (diameter = 16cm, height = 29cm) containing phosphoric acid. Temperature measurements were performed with an optical probe (Luxtron, LumaSense Technologies, Santa Clara, CA, USA) positioned in a small gel phantom with 3 wt.% Agar and 0.5 wt.% NaCl, while transmitting at maximum RF power of either the ^{1}H or ^{31}P frequency. Since there is no heat transfer through convection or perfusion in the gel phantom, this represents a worst-case situation compared to measurements *in vivo*. The gel phantom was positioned on spots that were suspected to carry locally high electrical fields, like ^{31}P detune circuits, ^{1}H traps and capacitors. Furthermore, the coil was checked by feeling by hand if any heating occurred on the housing of the insert.

The performance of the birdcage alone and the combined setup were tested with three healthy volunteers (2 female, aged: 28.3 ± 3.2 y) on a 3T MR-system (Magnetom Trio, Siemens Healthcare, Erlangen, Germany). The ^{31}P transmit efficiencies were compared by means of a slice selective pulse-acquire experiment (TR = 15 s) covering the brain, by assessing the voltage that corresponds to a γB_1 of 500 Hz, reflected by a maximized phosphocreatine (PCr) magnitude signal. ^{1}H transmit efficiencies were determined automatically by the MR system. To determine the noise correlation between the array elements, a single slice ^{31}P gradient-echo image was acquired while transmit power was set to zero.

A 3D MRSI free induction decay (FID) sequence with a WALTZ4 ^{1}H-decoupling scheme was used to acquire ^{31}P MR spectroscopic images of the whole brain for SNR comparisons between both coil setups. Repetition time (TR) was 2000 ms. For excitation a pulse with a duration of 500 µs and a flip angle of 40° (Ernst angle, assuming a maximum T_1 of 7500 ms) was applied. The dead time between pulse and acquisition was 100 μs. For 3D ^{31}P MRSI the FOV was set to 260x260x260 mm^3 applying Hamming-weighted k-space sampling, averaging 4 FIDs of 1024 data points around the center of a 10x10x10 k-space matrix. The voxel size defined as 64% of the point spread function area was approximately 40 cm^3 [16]. The measurement time was 13 minutes and 8 seconds. WALTZ4 ^{1}H-decoupling (γB_1 = 250Hz) was turned on during the first 256 ms (50%) of the acquisition window.

For ^{1}H SNR comparison, ^{1}H MR spectra of the anterior part of the occipital lobe were acquired with a single voxel point resolved spectroscopy (PRESS) sequence using CHESS water suppression [17, 18]. TR/TE were set to 3000/30 ms to measure a 20x20x16 mm^3 voxel with a flip angle of 90° (64 averages).

All volunteer studies were conducted with approval of the institutional review board of the Radboud university medical center Nijmegen.

Post processing

The amplitude and relative phase of the signal of each array coil element depends on the magnetization and the position of the excited volume with respect to the receive elements. As these parameters vary per array coil element, we used the WSVD algorithm for signal combination [15].

Before Fourier transform, the *in vivo* 3D ^{31}P MRSI data set was interpolated to a 16x16x16 matrix with a nominal voxel size of 16.25x16.25x16.25 mm^3. The SNR performance of the birdcage alone and the combination with the phased-array insert was evaluated in the center transversal partition of the 3D dataset in all volunteers. SNR was calculated as the ratio of the integral of the PCr peak as fitted by Metabolite Report in Syngo (work-in-progress package, Siemens Healthineers, Erlangen, Germany), divided by the standard deviation (SD) of the noise. Noise SD was calculated from a signal-free portion of the spectrum. An average noise correlation matrix was calculated from the noise in the ^{31}P gradient-echo images.

To evaluate the ^{1}H performance of the birdcage with and without the ^{31}P array inserted, the SNR of all single voxel ^{1}H spectra, acquired from the anterior part of the occipital lobe, were analyzed with LCModel software (v. 6.3-0C) using a simulated basis set of 24 metabolites [19]. SNR is

defined as the maximum of the N-acetylaspartate (NAA) signal at 2.01 ppm in the baseline-corrected spectrum divided by two times the root-mean-square of the residuals [20].

Results

To assess the performance of the ^{31}P receive head array we determined the Q-factor ratio Q_{UL}/Q_L for all individual array elements. The values for the Q ratio ranged from 1.4 to 2, depending on the head-to-element distance. Next, we determined the port-to-port (S21) decoupling, which ranged from -10 dB to -15 dB between neighboring elements and from -8.5 dB to -22.6dB for non-neighboring elements. The calculated noise correlation matrix showed variations in noise correlation between both neighboring and non-neighboring elements (Fig. 3).

To check whether SAR limits would be exceeded when transmitting with the birdcage coil in the combined coil configuration, temperature was measured at maximum transmit power of either the ^{1}H or ^{31}P frequency. This did not result in a temperature increase in the gel phantom, from which we conclude that the IEC limits were not exceeded. The temperature of the housing directly above the detuning circuits and cable traps was elevated but did not exceed 41°C. Based on these two results, the same SAR limits as used for the CE-approved ^{1}H/^{31}P birdcage coil could be applied to the combined setup.

The presence of the array coil did not cause any losses in ^{1}H transmit efficiency, whereas for the ^{31}P channel a 20% loss was observed, likely caused by the close proximity of the array electronics to the conductors of the birdcage. The SNR of ^{1}H and ^{31}P signals for the whole brain, as obtained from the NAA (2.01 ppm) and PCr signals respectively, was studied with the ^{1}H/^{31}P birdcage coil only and with a combination of this coil and the ^{31}P receive head-array insert.

The ^{1}H/^{31}P birdcage coil has a flat ^{31}P receive profile and the combined probe showed a ^{31}P profile with a radially increasing sensitivity from the center of the head towards the array elements. The SNR gain of the PCr peak due to the insertion of the ^{31}P array coil varied from 0.9 in the center up to a factor of 3.2 in the anterior part of the brain. The average SNR gain (± SD) of all selected voxels was 1.4 ± 0.4 (Fig. 4). The average linewidth (full width at half height) of PCr in the marked voxels of figure 4A, which include frontal brain areas, was 12.4 ± 7.5 Hz for the birdcage-only, and 14.4 ± 7.4 Hz in the combined setup.

To assess the ^{1}H MRS sensitivity for both coil configurations we used the SNR value of the NAA methyl peak at 2.01 ppm. For the birdcage, the ^{1}H SNR of a volume in the occipital lobe of the brain was 19, 20 and 17 for volunteers 1, 2 and 3 respectively. After inserting the ^{31}P head array, the SNRs were 20, 18 and 19. Ergo, the SNRs of ^{1}H MR spectra were not influenced by the presence of the ^{31}P array coil.

With a standard FID MRSI sequence, the resonances of phosphomonoesters, phosphodiesters and ATP are not well resolved due to ^{1}H-^{31}P J-coupling. Applying ^{1}H-decoupling can remove this heteronuclear coupling and results in well-resolved signals of phosphoethanolamine, phosphocholine, glycerophosphoethanolamine, glycerophosphocholine and ATP. ^{31}P signals were not affected by spurious signals or additional noise due to ^{1}H-decoupling (Fig. 5).

Discussion

In this work we combined a home-built ^{31}P 8-channel receive-array insert with a double-tuned ^{1}H/^{31}P birdcage transmit/receive coil to enable single-session combined ^{31}P and ^{1}H MRSI examinations without the need of repositioning the patient in clinical routine, trials and research at 3T.

Traditionally, ^{31}P MR spectroscopy and spectroscopic imaging have mostly been performed with surface coils. As RF transmit surface coils have an extremely inhomogeneous transmit field, the flip angles of conventional excitation pulses depend on the distance to the coil and need calibration. This can be largely overcome by adiabatic pulses [21]. However, these pulses require high power levels which makes it challenging not to exceed SAR limits, especially when techniques like ^{1}H-decoupling and ^{1}H-^{31}P NOE are applied. Our combined coil configuration takes advantage of separated transmit and receive elements. This allows us to generate a homogeneous transmit field with the volume ^{1}H-^{31}P birdcage coil and to achieve a high sensitivity close to the array coil. For excitation, this allows to employ rectangular pulses at lower RF power. Since shorter repetition times can be achieved with rectangular pulses, flip angle calibration can be performed fast, and more averages with small flip angles can be acquired in the same amount of time, resulting in a higher SNR per unit time.

With the head-array coil insert we achieved an up to 3.2-fold increase in SNR in superficial anterior brain areas compared to the birdcage coil alone, while almost maintaining similar SNR in the center of the brain. This SNR profile is in line with other studies using an array of coils [9, 22].

Noise correlation values of the array coil ranged from 0.05 up to 0.66 with a mean of 0.31 ± 0.16. This is comparable to reported values of a commercially available 8-channel ^{1}H coil [23], but higher than reported for other ^{31}P and ^{1}H home-built coils: 0.1 [11] and 0.12 [23]. The Q_{UL}/Q_{L} ratio of an unloaded single element is approximately halved when it is placed inside the

birdcage. The ratio also depends on the element position in the birdcage, which implies a shared mutual resistance. Furthermore, with both the 8-channel array and a sample present inside the birdcage, location-dependent coupling caused extra inter-element coupling of the array elements. A better decoupling between birdcage and receive elements would further improve the performance of the array. However, it was not possible to make modifications to the commercial coil for safety and regulatory reasons.

Even though the maximum γB_1 for ^{31}P of the birdcage was reduced by ~20% in the presence of the array coil, the probe was still capable of generating a 90^0 flip angle with a bandwidth of approximately 48 ppm, which is sufficient to excite all ^{31}P spins relevant for *in vivo* applications [24].

Conclusion

The combination of an 8-channel ^{31}P head array with a double-tuned $^{31}P/^{1}H$ birdcage offers the advantages of an increase in ^{31}P SNR, while retaining a homogeneous transmit field on both frequencies. The losses in ^{1}H performance and the ^{31}P-transmit performance of the birdcage were negligible or could be overcome. Our setup facilitates combined *in vivo* ^{1}H and ^{31}P MRSI examinations on a clinical 3T system without repositioning the subject. The proposed coil configuration in this study paves the way for human applications at 3T with more advanced sequences like sRINEPT (selectively refocused insensitive nuclei enhanced by polarization transfer) [25]. Another future perspective for the probe is the possibility of more efficient and informative data sampling by interleaved ^{31}P and ^{1}H MRS acquisitions on current state-of-the-art MR-systems.

Acknowledgements

We thank A. Veltien for the technical discussions about safety an design of the receive array and E.W.J. Philips for implementing the WSVD code into the pulse sequence, C. Rodgers is funded by the Wellcome Trust and the Royal Society (Grant Number 098436/Z/12/Z).

Figures and tables

Figure 1. Overview of the combined coil configuration:

The ^{31}P 8-channel head-array coil is positioned inside a commercially available, detunable ^{1}H/^{31}P birdcage. The insert is connected to the MR system via a custom-built ^{31}P interface. The frontal element at the side of the patient's face is smaller than the other 7 elements to maximize the subject's comfort.

Figure 2. Diagram of ^{31}P head array electric circuit:

Detailed overview of all components of the anterior element, the connection to the interface, and the components of the interface electronics. The component functions are indicated as: decoupling capacitor (Cdec), tuning capacitors (Ct), matching circuit (Cm, Lm), RF-block inductors (Ldc), ^{31}P active detuning circuit (Ldet, Cdet), improved ^{1}H trap circuits (Cs, Cp, Ltr), PIN-diodes (PIN), ^{1}H tank circuit (Lta, Cta) and the phase shifter (Lph, Cph).

Figure 3. Noise correlation map of the ^{31}P head-array elements.

The noise correlation map was calculated from gradient-echo data. On the vertical and the horizontal axis are the element numbers. The red gapped circle represents the element numbering of the head array as seen from the feet side.

Figure 4. SNR gain by the ^{31}P head array.

A transversal image of the brain with a region of interest (yellow line) and an overlay of corresponding MRSI voxel numbers **(A)**. The SNR in the ROI is represented row-wise and per volunteer in **(B)**. Voxels of the second row are marked with a yellow bar. Line colors represent the different volunteers. The average SNR of all volunteers is projected on the brain image in **(C)** and is presented row-wise (± SD) in (**D**).

Figure 5. Examples of ^{31}P and ^{1}H spectra acquired with the birdcage only and combined with the phased array insert.

Indication of ^{1}H (blue) and ^{31}P (red) voxel positioning in a transversal and sagittal slice of the brain **(A)**. ^{31}P **(B)** and ^{1}H **(C)** spectra were acquired without (left column) and with (right column) the insert array. Both ^{1}H spectra were received with the birdcage. ^{31}P spectra were acquired with WALTZ4 ^{1}H-decoupling. Resolved signals of phosphoethanolamine (PE), phosphocholine (PC), inorganic phosphate (Pi), glycerophosphoethanolamine (GPE) and

glycerophosphocholine (GPC), phosphocreatine (PCr) and adenosine triphosphate (ATP) are indicated in the ^{31}P spectra. In the ^{1}H spectrum total choline (tCho), total creatine (tCr) and N-acetylaspartate (NAA) are marked.

1. Mandal, P.K., *Magnetic resonance spectroscopy (MRS) and its application in Alzheimer's disease.* Concepts in Magnetic Resonance Part A, 2007. **30A**(1): p. 40-64.
2. Maintz, D., et al., *Phosphorus-31 MR spectroscopy of normal adult human brain and brain tumours.* NMR Biomed, 2002. **15**(1): p. 18-27.
3. Pettegrew, J.W., et al., *Alterations of cerebral metabolism in probable Alzheimer's disease: a preliminary study.* Neurobiol Aging, 1994. **15**(1): p. 117-32.
4. van der Grond, J., et al., *Regional distribution of interictal 31P metabolic changes in patients with temporal lobe epilepsy.* Epilepsia, 1998. **39**(5): p. 527-36.
5. Oz, G., et al., *Clinical proton MR spectroscopy in central nervous system disorders.* Radiology, 2014. **270**(3): p. 658-79.
6. Matson, G.B., P. Vermathen, and T.C. Hill, *A practical double-tuned 1H/31P quadrature birdcage headcoil optimized for 31P operation.* Magn Reson Med, 1999. **42**(1): p. 173-82.
7. Greenman, R.L. and R. Rakow-Penner, *Evaluation of the RF field uniformity of a double-tuned 31P/1H birdcage RF coil for spin-echo MRI/MRS of the diabetic foot.* J Magn Reson Imaging, 2005. **22**(3): p. 427-32.
8. Vaughan, J.T. and J.R. Griffiths, *RF Coils for MRI*. 2012.
9. Avdievich, N.I. and H.P. Hetherington, *4 T Actively detuneable double-tuned 1H/31P head volume coil and four-channel 31P phased array for human brain spectroscopy.* J Magn Reson, 2007. **186**(2): p. 341-6.
10. Lakshmanan, K., et al., *An eight-channel sodium/proton coil for brain MRI at 3T.* Nmr in Biomedicine, 2018. **31**(2).
11. van de Bank, B.L., et al., *Optimized (31)P MRS in the human brain at 7 T with a dedicated RF coil setup.* NMR Biomed, 2015. **28**(11): p. 1570-8.
12. Wang, J., *A novel method to reduce the signal coupling of surface coils for MRI.* Proceedings of the 4th Annual Meeting of ISMRM, New York, 1996, 1996. **4**: p. 1434.
13. Roemer, P.B., et al., *The NMR phased array.* Magn Reson Med, 1990. **16**(2): p. 192-225.
14. Meyerspeer, M., et al., *An improved trap design for decoupling multinuclear RF coils.* Magn Reson Med, 2014. **72**(2): p. 584-90.
15. Rodgers, C.T. and M.D. Robson, *Receive array magnetic resonance spectroscopy: Whitened singular value decomposition (WSVD) gives optimal Bayesian solution.* Magn Reson Med, 2010. **63**(4): p. 881-91.
16. Pohmann, R. and M. von Kienlin, *Accurate phosphorus metabolite images of the human heart by 3D acquisition-weighted CSI.* Magn Reson Med, 2001. **45**(5): p. 817-26.
17. Bottomley, P.A., *Spatial localization in NMR spectroscopy in vivo.* Ann N Y Acad Sci, 1987. **508**: p. 333-48.
18. Haase, A., et al., *1H NMR chemical shift selective (CHESS) imaging.* Phys Med Biol, 1985. **30**(4): p. 341-4.
19. Provencher, S.W., *Estimation of metabolite concentrations from localized in vivo proton NMR spectra.* Magn Reson Med, 1993. **30**(6): p. 672-9.
20. Provencher, S., *LCModel & LCMgui User's Manual*. 2016.
21. Garwood, M. and L. DelaBarre, *The return of the frequency sweep: designing adiabatic pulses for contemporary NMR.* J Magn Reson, 2001. **153**(2): p. 155-77.
22. Pinkerton, R.G., E.A. Barberi, and R.S. Menon, *Transceive surface coil array for magnetic resonance imaging of the human brain at 4 T.* Magn Reson Med, 2005. **54**(2): p. 499-503.
23. Wiggins, G.C., et al., *32-channel 3 Tesla receive-only phased-array head coil with soccer-ball element geometry.* Magn Reson Med, 2006. **56**(1): p. 216-23.
24. De Graaf, R.A., *In vivo NMR spectroscopy : principles and techniques*. 2nd ed. 2007, Chichester, West Sussex, England ; Hoboken, NJ: John Wiley & Sons. xxi, 570 p., 8 p. of plates.
25. Klomp, D.W., et al., *Efficient 1H to 31P polarization transfer on a clinical 3T MR system.* Magn Reson Med, 2008. **60**(6): p. 1298-305.

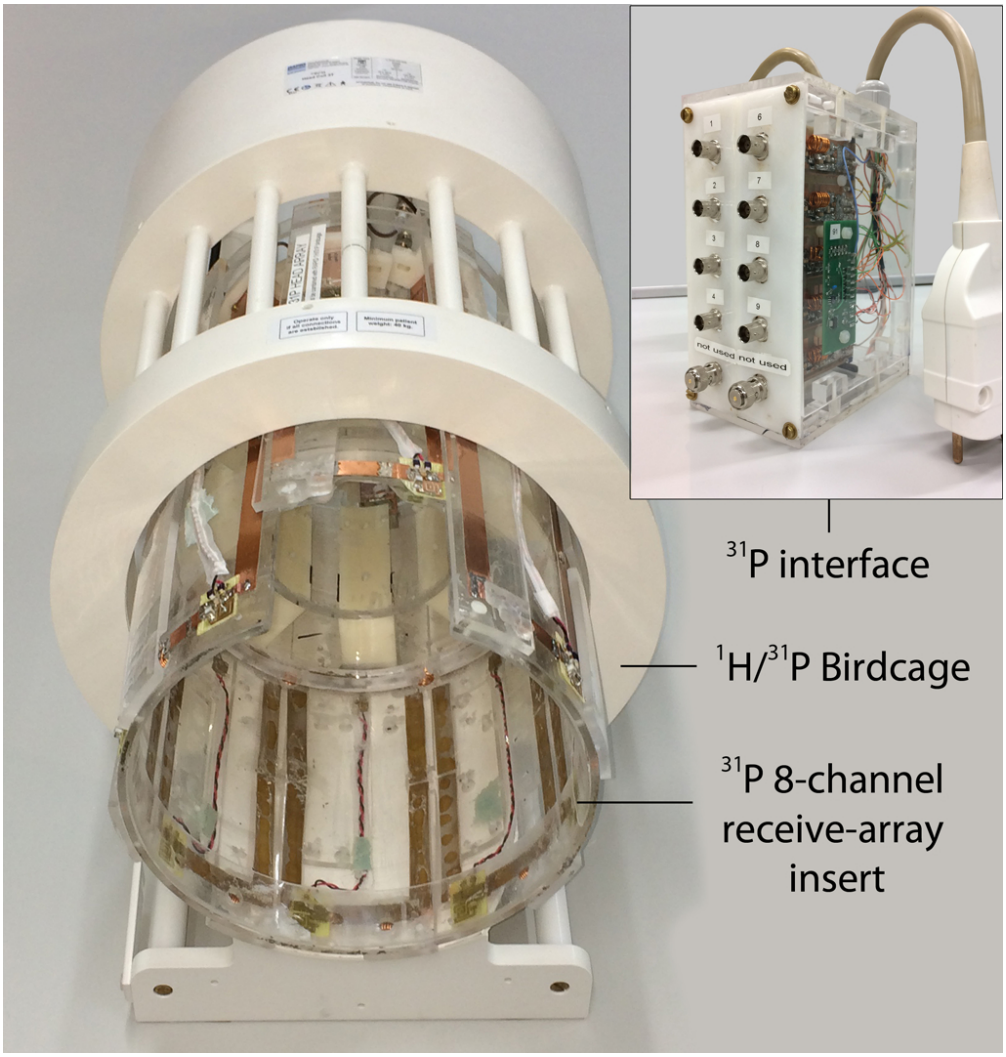

Figure 1. Overview of the combined coil configuration. The ^{31}P 8-channel head-array coil is positioned inside a commercially available, detunable ^{1}H/^{31}P birdcage. The insert is connected to the MR system via a custom built ^{31}P interface. The frontal element at the side of the patient's face is smaller than the other 7 elements to maximize the subject's comfort.

86x90mm (300 x 300 DPI)

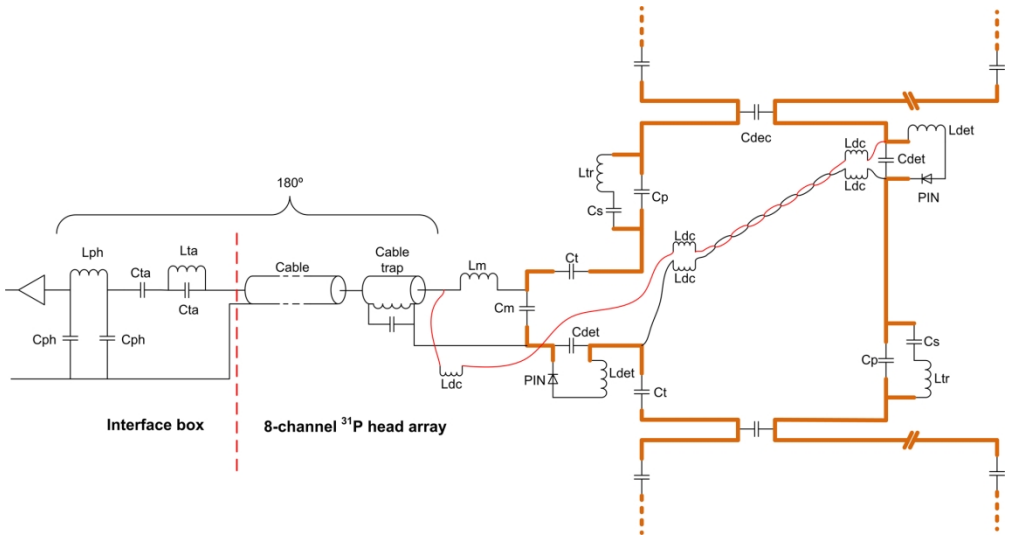

Figure 2. Diagram of ^{31}P head array electric circuit: Detailed overview of all components of the anterior element, the connection to the interface, and the components of the interface electronics. The component functions are indicated as: decoupling capacitor (C_{dec}), tuning capacitors (C_t), matching circuit (C_m, L_m), RF-block inductors (L_{dc}), ^{31}P active detuning circuit (L_{det}, C_{det}), improved ^{1}H trap circuits (C_s, C_p, L_{tr}), PIN-diodes (PIN), ^{1}H tank circuit (L_{ta}, C_{ta}) and the phase shifter (L_{ph}, C_{ph}).

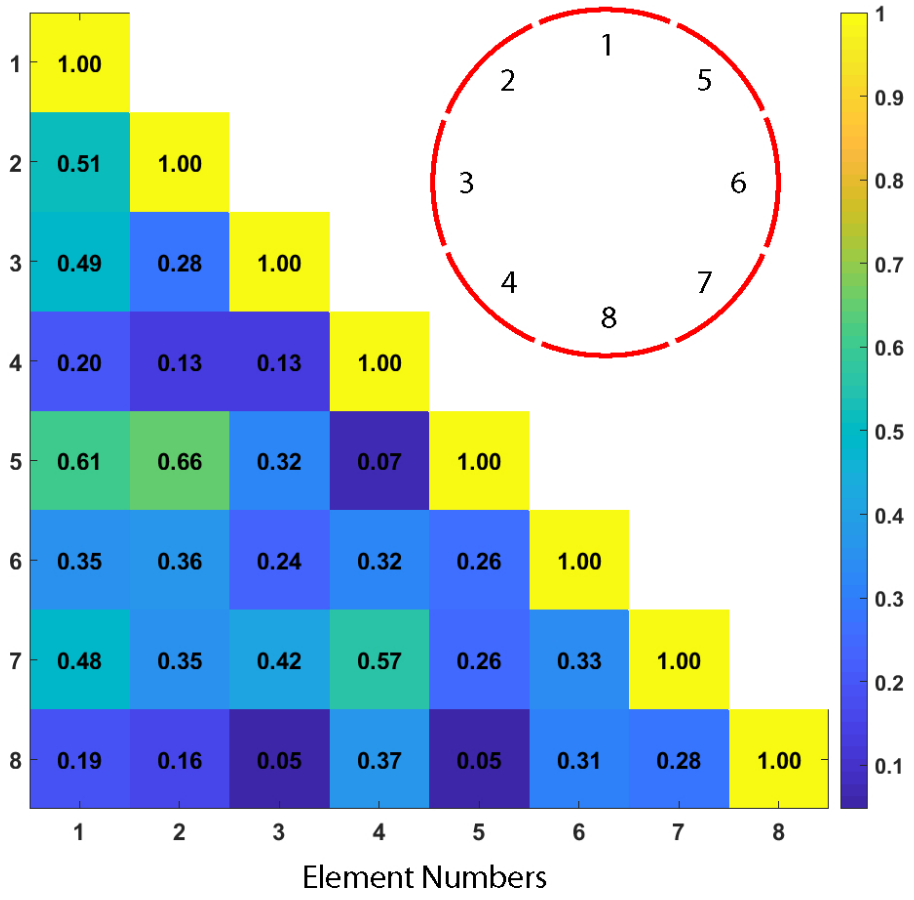

Figure 3. Noise correlation map of the ^{31}P head-array elements. The noise correlation map was calculated from gradient echo data. On the vertical and the horizontal axis are the element numbers. The red gapped circle represents the element numbering of the head array as seen from the feet side.

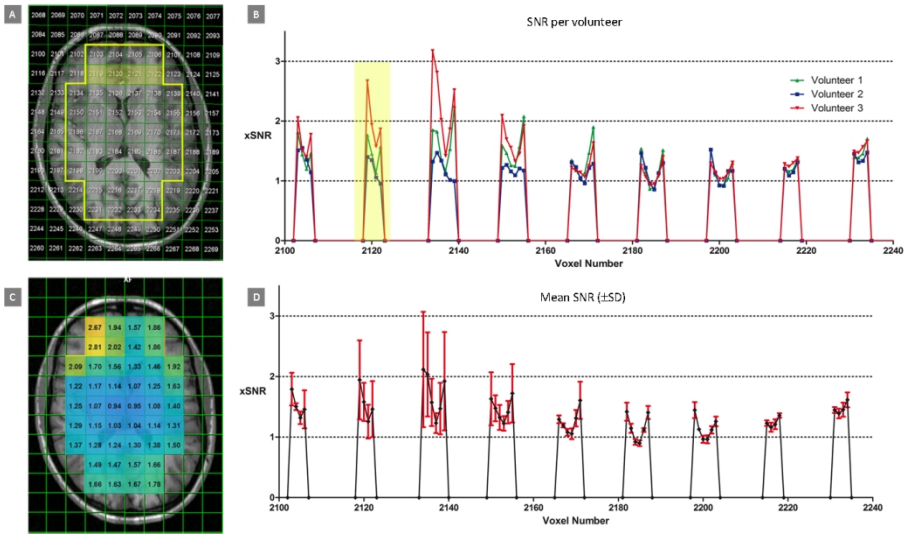

Figure 4. SNR gain by the ^{31}P head array. A transversal image of the brain with an region of interest (yellow line) and an overlay of corresponding MRSI voxel numbers **(A)**. The SNR in the ROI is represented row-wise and per volunteer in (**B**). Voxels of the second row are marked with a yellow bar. Line colors represent the different volunteers. The average SNR of all volunteers is projected on the brain image in (**C**) and is presented row-wise (± SD) in (**D**).

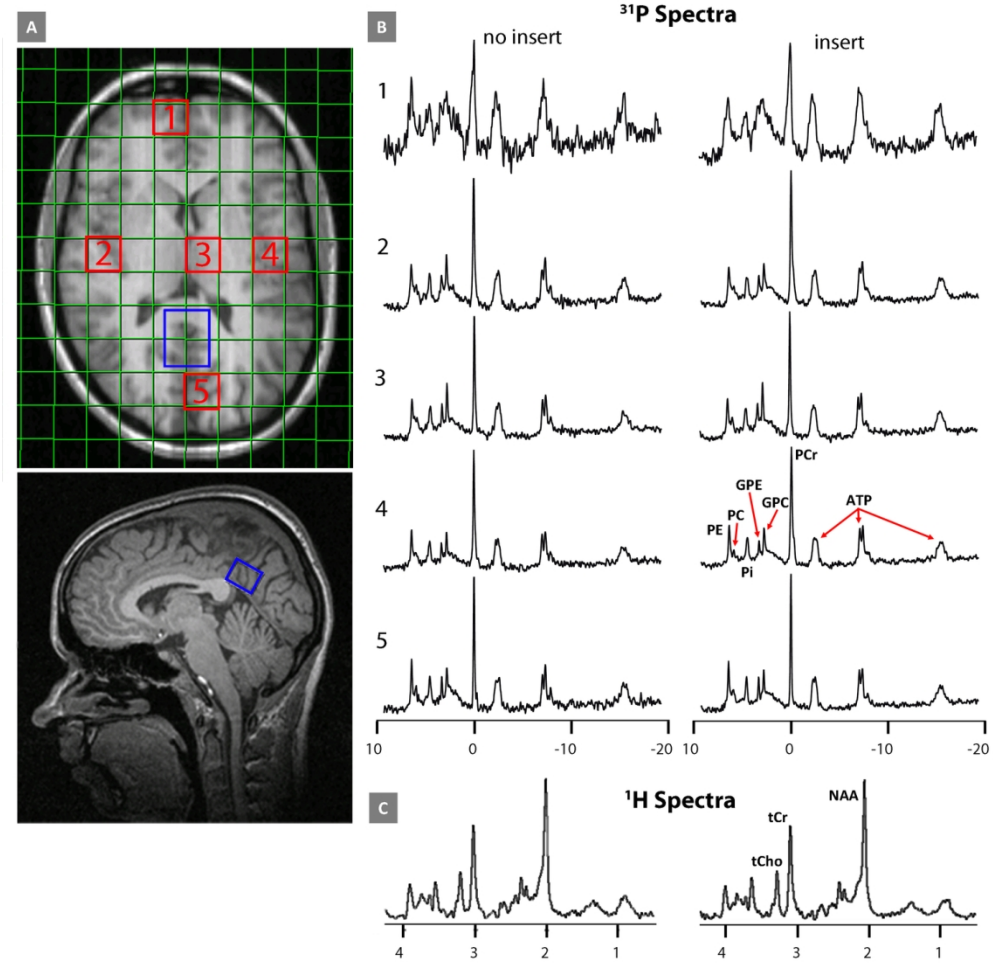

Figure 5. Example of ^{31}P and ^{1}H spectra acquired with the birdcage only and combined with the phased array insert. Indication of ^{1}H (blue) and ^{31}P (red) voxel positioning in a transversal and sagittal slice of the brain **(A)**. ^{31}P **(B)** and ^{1}H **(C)** spectra were acquired without (left column) and with (right column) the insert array. Both ^{1}H spectra were received with the birdcage. ^{31}P spectra were acquired with WALTZ4 ^{1}H decoupling. Resolved signals of phosphoethanolamine (PE), phosphocholine (PC), inorganic phosphate (Pi), glycerophosphoethanolamine (GPE) and glycerophosphocholine (GPC), phosphocreatine (PCr) and adenosine triphosphate (ATP) are indicated in the ^{31}P spectra. In the ^{1}H spectrum total choline (tCho), total creatine (tCr) and N-acetylaspartate (NAA) are marked.

130x127mm (300 x 300 DPI)